Manipulation of Crystallization Sequence in PEO-*b*-PCL Films Using Solvent Interactions

Natasha Brigham, Christopher Nardi, Allison Carandang, Kristi Allen, Ryan M. Van Horn*

Department of Chemistry, Allegheny College, Meadville, PA 16335
KEYWORDS. Diblock copolymers, crystallization, solvent interactions.

ABSTRACT: The physical structure of polymer films is important for understanding the observed macroscopic properties. In crystalline-crystalline block copolymers, the hierarchical nature of assembly is even more influential. Controlling this assembly process is crucial for tailoring film properties. In materials where crystallization of each block occurs nearly simultaneously, the ability to manipulate crystallization order is desirable. Poly(ethylene oxide)-*b*-poly(ε-caprolactone) (PEO-*b*-PCL) films were monitored *via* ATR-FTIR to determine the crystallization order during drying from varying solvents. PCL crystallized first from most solvents except toluene and ethyl acetate, where PEO nucleation occurred first. Moreover, after melting the sample to remove solvent-polymer interaction effects, PCL was first to crystallize from the melt, as has been previously reported. Differences in the films' morphologies based on crystallization order were observed using polarized optical microscopy. These results demonstrate that the order of crystallization and the assembly within the film was controllable when casting symmetric diblock PEO-*b*-PCL films from different solvents.

INTRODUCTION

Diblock copolymers have become prevalent in research over the last several decades because of their applications in nearly all of the materials industry. Copolymers are of interest due to their ability to combine two polymers with different characteristics into one large molecule with a combination of each polymer's respective properties. Diblock copolymers can contain chains that are semi-crystalline (C) or amorphous (A); therefore, three different combinations of copolymers are possible: crystalline-crystalline (CC), amorphous-crystalline (AC), or amorphous-amorphous (AA). Depending on the type of diblock copolymer, a wide array of properties exists. Because there is a large volume of research on these types of materials, only relevant CC copolymers will be discussed.

The order in which CC diblock copolymers crystallize has an impact on characteristics of the polymeric material. In most copolymers, the crystallization occurs in a sequential manner due to the vast difference in melting temperatures (T_m) of each block.[1-11] The initial nucleation of one block leads to imperfect or confined crystallization of the other, therefore resulting in a structure that is more crystallized with the first block.[1,9,11-17] When strongly-segregated materials undergo microphase separation, this structural element also influences the crystallization and the macroscopic behavior.[18-20] Thermodynamically, the stability of the amorphous melt for the high T_m block decreases more rapidly during cooling, leading to crystal nucleation and subsequent growth of those crystals prior to nucleation of the second block. The lower T_m block crystallizes after further cooling, typically at a temperature much lower than the first block, either in a microphase-separated domain in strongly-segregated block copolymers[21-23] or between the lamellae of the crystals formed by the higher T_m block (weakly-segregated or miscible).[22-24] For these more common CC block copolymers, the macroscopic properties are derived primarily from the higher T_m polymer crystals and

hierarchical organization. Control over the crystallization processes is difficult because the window to manipulate morphology, crystallinity, and other structural aspects that govern properties is limited and isolated to each individual block.

With certain copolymers, crystallization occurs nearly simultaneously, or coincidently, due to similar melting temperatures.[21, 25-28] Controlling the order of crystallization, or nucleation, in these cases becomes a matter of enabling an environment to favor one block crystallizing over the other *via* factors such as molecular weight,[28-29] thermal history,[30,31] solvent,[32-34] atmosphere,[35-37] or others. Here, the ability to manipulate the crystallization behavior is more robust as it is possible to influence morphology, crystallinity, etc. by controlling the assembly structure, order of crystallization, and crystallization kinetics. Thermodynamically, the stabilities of the amorphous melts are more similar. By stabilizing, or destabilizing, one melt preferentially (or destabilizing the formation of crystal nuclei with diluent[38-39] or confinement effects[2]), crystal structure development can undergo dramatic changes. Thus, it is possible to create materials of identical chemical composition that display different properties *via* structural changes in the assembly of the molecules. While the phenomenon of coincident crystallization has been observed in several block copolymers,[40-42] a deep understanding of its origin, the thermodynamic and kinetic reasons for observed behavior, and technological advances in tailoring it have not been studied as extensively.

Poly(ethylene oxide)-*b*-poly(ε-caprolactone) (PEO-*b*-PCL) is a miscible, or weakly-segregated, diblock copolymer of which melt crystallization occurs with the larger block first[39,43-47] and exhibits coincident crystallization at similar weight fractions though PCL nucleates first.[1,25,28,33,40,44-47] Being able to control the properties of this copolymer is crucial for its biomedical applications. Though molecular weight and thermal history are widely studied to control the crystallization process, solvent primarily only has been studied in the

area of micelle formation for these copolymers.[48-50] For example, as described by Yu *et al.*[50] in their work with PEO-*b*-PCL micelles, the polymer–solvent interactions determined the composition and magnitude of both the core and the corona of the micelle, as the solvent forced the polymer with unfavorable interactions into the core. This same idea can be applied to other mechanisms of crystallization. In solution crystallization, for example, if one block of the copolymer does not want to interact with the solvent, then, it will crash out of solution and crystallize. This was exhibited by Van Horn *et al.*[51] with *n*-hexanol and amyl acetate for a 13k-9k g/mol molecular weight sample of PEO-*b*-PCL. When the polymer was dissolved and crystallized in amyl acetate, PEO single crystals were observed and confirmed by electron diffraction. In *n*-hexanol, PCL single crystals were observed. These results confirm the idea that using a certain solvent preferentially crystallized one of the blocks. It is assumed, therefore, that these preferential solvent interactions should govern crystallization in casted block copolymer films by either causing pre-organization of the chains in solution or by selectively solvating (or selectively precipitating) one block during drying of the film.

In this research, we intend to show that casting solvent affects the order of crystallization and crystal development in polymer films. A symmetric 10.0k-10.3k g/mol PEO-*b*-PCL (w_{PCL} = 0.51) sample was used to yield more meaningful insight to the direct solvent effects on the sequence of crystallization of the diblock copolymer because of its coincident crystallization mechanism. Using a symmetric copolymer, the effect of molecular weight on the crystallization process becomes diminished, i.e. larger block nucleates and/or crystallizes first, and solvent effects on the sequence are observed more effectively. The crystallization order was monitored using solution crystallization and ATR-FTIR techniques. The role of solvent effects on crystal morphology in PEO-*b*-PCL films was addressed as well.

EXPERIMENTAL SECTION

Materials. A 10,000 g/mol-10,300 g/mol (10k-10.3k, PDI = 1.15) sample of poly(ethylene oxide)-*b*-poly(ε-caprolactone) (PEO-*b*-PCL) was purchased from Advanced Polymer Materials Inc. and used as received. The molecular weight ratio was verified using ^{1}H NMR analysis. Solvents (amyl acetate, acetone, chloroform, hexyl alcohol, ethyl acetate, ethyl formate, methyl ethyl ketone and toluene) were purchased from EMD Chemicals and Fisher Chemicals and were not further purified, unless otherwise stated.

Sample Preparation. 1% by weight solutions of 10k-10.3k PEO-*b*-PCL were prepared in acetone, chloroform, ethyl acetate, ethyl formate, methyl ethyl ketone (MEK), and toluene. Samples were heated to between 40°C and 60°C to dissolve the polymer in all solvents except chloroform. The solutions stayed homogeneous after cooling to room temperature as confirmed by visual inspection; however, the polymer precipitated from ethyl acetate, ethyl formate, and MEK if cooled below 22°C. Films of these solutions were prepared for attenuated total reflectance (ATR) FTIR spectroscopy and optical microscopy. For ATR-FTIR, the solution was cast onto the ATR crystal, and the solvent was allowed to evaporate, leaving a film. For the solvents that precipitated near room temperature, the solutions were casted warm onto the ATR stage to prevent precipitation. Films also were prepared by drop-casting 200 μL of solution onto glass slides for polarized optical microscopy (POM) or KBr salt plates for transmission FTIR. All films were estimated to be greater than 2 μm thick; therefore, film thickness effects on crystallization should be minimized.

*Solution Crystallization***.** 0.01% by weight solutions of 10k-10.3k PEO-*b*-PCL were dissolved in either *n*-hexanol or amyl acetate at 60°C and were left to sit at room temperature overnight until a precipitate formed. The precipitate was disaggregated by shaking the solution. 10 μL

of solution then was placed onto a glass slide and analyzed using optical microscopy. The same process was done for ethyl acetate (1% solution), methyl ethyl ketone (0.01% solution), and ethyl formate (0.01% solution) to check for single crystal formation of either block. These samples were cooled below room temperature in a refrigerator to form a precipitate. The precipitate was prepared on slides in the refrigerator as well to prevent dissolution during drying.

*Optical Microscopy***.** A Leica DM2700P optical microscope (OM) with a CCD camera was used to visualize crystallized structures from different solvents. For solution crystallization, bright-field images were obtained to visualize the single crystal morphology. Film crystal morphologies were identified using the Leica DM2700P with the polarizer/analyzer and a quarter-wave retardation plate.

ATR and Transmission FTIR. FTIR analysis was performed on a Nicolet 6700 FTIR with a Smart iTR single bounce attachment (diamond crystal) for ATR studies to monitor crystallization of each block in the copolymer. The resolution and number of scans were both set to 8 to maintain a short spectral accumulation time. 200 μL of 1% by weight solutions were placed onto the ATR crystal. Spectra were taken at regular intervals to monitor the crystallization order during drying. Dried films on KBr salt plates prepared by the same procedure were analyzed via transmission FTIR after several hours of drying to confirm crystallization of both blocks, to compare relative crystallinities of each block, and to identify any morphological differences through vibrational bands which are parallel or perpendicular to the crystal's chain (or *c*) axis.

In both the ATR and transmission arrangements, the following bands were used to detect crystallization during drying: 842, 1061, and 1280 cm^{-1} for the PEO block,[52] and 731, 1045,

1192, 1295, and 1725 cm^{-1} to identify the crystallization of PCL.[53-54] Specifically, amorphous PCL appeared at 1735 cm^{-1} and shifted to a band centered at 1725 cm^{-1} when crystallization began due to a change in the C=O bond stretching.[53-54] The appearance of these bands demonstrated the time at which either block began to crystallize, therefore, suggesting the order of crystallization in the diblock. A summary of all relevant bands is shown in Table 1. Once dried, ATR samples were heated with a hot gun until fully melted (above 70°C), as indicated by spectral data. During the cooling of the film, spectra were taken, and the bands were monitored to check for crystallization of PEO or PCL. Each sample was melted five times to ensure the absence of solvent effects.

Table 1. Summary of the relevant peaks and their functionalities used to indicate PEO and PCL crystallization (from References 52-54)

Crystalline band (cm^{-1})	Represented block	Assignment	Chain axis orientation	Correlated amorphous band (cm^{-1})
731	PCL	$\rho(CH_2)$		--
842	PEO	$\rho(CH_2)$		856
963	PCL & PEO	$\rho(CH_2)$	//	--
1045	PCL	$\rho(CH_2)$	//	1040
1061	PEO	$\nu_a(OCO)$	$\perp$	--
1192	PCL	$\nu(OCO)$	//	1170
1280	PEO	$\tau_a(CH_2)$	$\perp$	--
1295	PCL	$\nu(CO) + \nu(CC)$	//	--
1343	PEO	$\omega_a(CH_2)$	//	1350
1362	PEO	$\omega_s(CH_2)$	$\perp$	1350
~1470	PCL & PEO	$\delta_a(CH_2)$	$\perp$	1460
1725	PCL	$\nu(C=O)$		1734

RESULTS AND DISCUSSION

To prove the principal that the order of crystallization can be controlled *via* solvent effects in the 10k-10.3k symmetric PEO-*b*-PCL diblock copolymer, a replicate of the work done by Van Horn *et al.*[51] was applied; amyl acetate and *n*-hexanol were used to induce solution crystallization of either block. Based on solvent affinity, it was suggested that amyl acetate is a poorer solvent for PEO, and therefore, will allow for it to crash out of solution and form solution-grown PEO single crystals. On the contrary, *n*-hexanol was shown to be a poorer solvent for PCL and would make it crash out of solution first, causing PCL single crystals to be present in solution. Both these theories were demonstrated to be true for 10k-10.3k PEO-

b-PCL 0.01% (w/w) solutions. These solution were heated to 65°C dissolve the polymer and cooled to room temperature until a precipitate formed. After formation of a cloudy solution, the precipitate was analyzed using optical microscopy (OM). The OM results are shown in Figure 1. These images mimic the findings in the literature due to the appearance of matching single crystal morphology in corresponding solvents: hexagonal (truncated lozenge) crystals for PCL (Fig. 1a) and squares for PEO crystals (Fig. 1b).[51] In both cases, the non-single crystal block is confined to the basal surface of the single crystals.[51, 54-56] This observation is proof of the principle that solvent could be used to effectively control the order of crystallization in a symmetric diblock containing two polymers of almost equal melting temperatures.

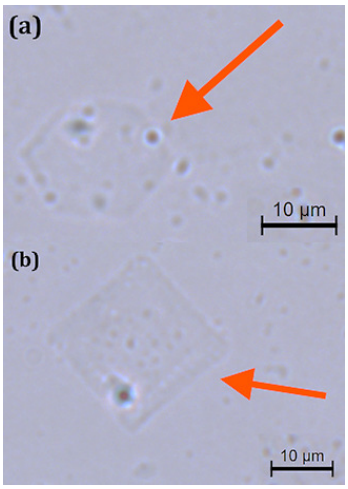


Figure 1. Optical microscope images of 10k-10.3k PEO-*b*-PCL crystals (a) PCL single crystal from *n*-hexanol and (b) PEO single crystal from amyl acetate. The second block is confined to the basal surfaces of these crystals.

Although here, the crystallization occurs in solution, the same principle should apply to drying from solvent casting. In solution crystallization, poor solubility at room temperature is desired to facilitate crystal formation. For films, as the solvent evaporates, one block should preferentially phase separate from the solvent due to unequal solubility parameters. The selective solubility concept should be relevant even for solvents that dissolve the PEO-*b*-PCL sample at room temperature, where the more soluble block can facilitate the dissolution of

the less soluble block. These types of solvents are more relevant for processing PEO-*b*-PCL films on a larger scale.

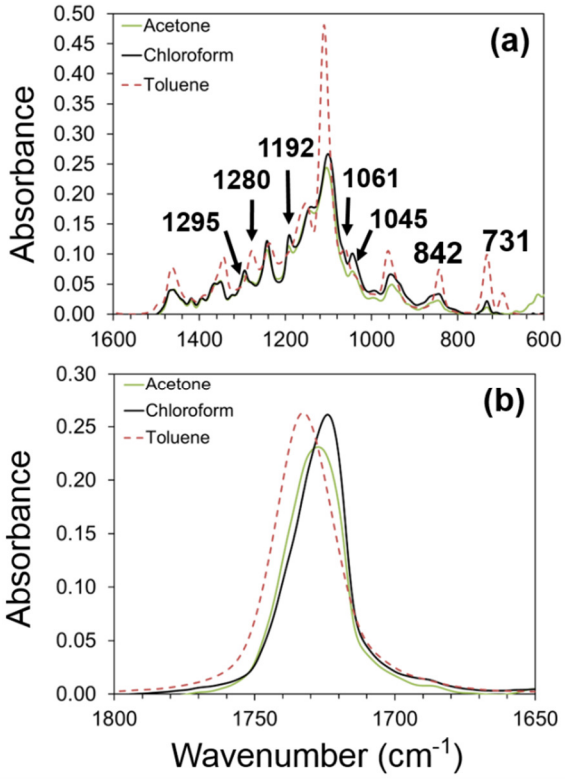


Figure 2. Overlayed ATR-FTIR spectra of 10k-10.3k PEO-*b*-PCL samples cast from chloroform (black line), acetone (green line), and toluene (dashed red line). The spectra range from 600 to 1600 cm^{-1} (a) and from 1650 to 1800 cm^{-1} (b). The dashed line represents spectra in which PEO has crystallized first during drying.

Common Solvents. Three solvents that were used in this research, acetone, chloroform, and toluene, are common solvents for polymer film preparation. It should be noted that both acetone and toluene were heated to 40°C to dissolve the powder but remained homogeneous by visual inspection after cooling to room temperature. For these solvents, getting either block to form solution-grown single crystals was difficult without significant cooling. While this experiment would complement the analysis from Figure 1, our interest is in film crystallization; therefore, solution crystallization was not the preferred method of analysis. Instead, ATR-FTIR was used to monitor crystallization of each block in the

copolymer during drying. Spectra were taken at regular intervals (~20 sec) to monitor the crystallization order. To identify crystallization order, a number of bands were utilized. For PCL crystallization, a band appearance at 731, 1045, 1192, and/or 1295 cm^{-1} and a shift in the 1734 cm^{-1} (amorphous PCL) band to the band centered at 1725 cm^{-1} (crystalline PCL) suggested that PCL was in a crystalline phase. The relevant bands that indicate PEO has crystallized include appearances of bands at 842, 1063, and 1280 cm^{-1}. These peaks were shown above in Table 1. Depending on which set of bands appear or shift first, information on the block that crystallized first was obtained. For clarity and accuracy, all the available peaks were monitored in order to avoid convolution with any solvent peaks or any effects due to chain orientation. With the ATR attachment, the material near the ATR crystal surface was probed preferentially; however, we will show that this and the wavelength dependence of evanescent wave propagation are inconsequential to identifying nucleation of a given block.

Figure 2 shows the ATR-FTIR spectra of 10k-10.3k PEO-*b*-PCL films cast from acetone (green line), chloroform (black line) and toluene (dashed red line) during drying. The data presented in Figure 2 only shows the first indication of PEO crystallization (dashed lines) or first indication of PCL crystallization (solid lines). Figure 2a is the spectral range from 600 cm^{-1} to 1500 cm^{-1}, and the bands of interest for PCL crystallization (731, 1045, 1192, and 1295 cm-1) and PEO crystallization (842, 1061, and 1280 cm-1) are labeled for clarity. For brevity, only the first appearance of crystallization is shown; the absence of crystalline bands for the block that crystallizes second is proof of crystallization order. All spectra were normalized by the total area of the bands at 1700 cm^{-1} (1734 cm^{-1} for amorphous PCL and 1725 cm^{-1} for crystalline PCL) as seen in Figure 2b since the total amount of PCL should be comparable for all films. This technique was applied to all FTIR analyses to make the visual comparisons more clear. ATR-FTIR spectra for homopolymer PEO, homopolymer PCL, and all solvents

used in this study can be found in the Supporting Information (Figure S1). Additionally, a series of spectra showing the drying process for solvents MEK and ethyl formate, which will be discussed in the next section, have been included in Figure S2. These figures are provided to demonstrate that the bands associated with the solvent are small, if present, once crystallization begins, with the exception of toluene. Somewhat surprisingly, amorphous bands were observed during drying, which indicates that although solvent bands were not observed due to the polymer spectra's dominance, the polymer, or the individual block must still be solvated since drying occurred below the crystallization temperature. Finally, the identified bands herein are clear evidence that nucleation/growth has occurred in one block prior to the other since there is no overlap with solvent or the other polymer block.

According to Figure 2, when using chloroform or acetone for the casting solvent, the solid line spectra showed growth of the bands associated with PCL crystallization, namely 731, 1045, 1192, and 1295 cm^{-1} in Figure 2a and the beginning of the shift of the 1734 cm^{-1} band to 1725 cm^{-1} in Figure 2b before any PEO bands (842 and 1280 cm^{-1} are most obvious) appeared. Given these spectra, PCL was crystallized first in these two solvents. Thus, chloroform and acetone provided similar nucleation and crystallization order as compared to the melt.[25,30,58-61] Casting the diblock from a toluene solution showed, for the first time, that PEO was crystallized first. This is visualized in Figure 2 by the red dashed line where the start of the growth of the 842, 1061, and 1280 cm^{-1} bands occurred before any of the indicated PCL bands began to crystallize. Other bands at 963 and 1470 cm^{-1} seem to indicate PEO crystallization as well; however, there are contributions from both blocks at these wavenumbers (Table 1). Because of this overlap, they will not be used to identify crystallization of one block over the other to avoid possible convolution. The large bands at 700 cm^{-1} and 730 cm^{-1} is representative of toluene in this case and was proven by taking a

spectrum of just toluene (Figure S1). No other bands present in Figure 2a are associated with toluene. Because of the overlap, the PCL band at 731 cm^{-1} is not preferable to identify PCL crystallization. However, all other PCL bands, where solvent overlap does not occur, indicate that PCL is amorphous. The crystalline PCL band at 1725 cm^{-1} has not appeared, and the amorphous band at 1734 cm^{-1} is still present. Figure 2 provides evidence that using different solvents allows for control of PEO-*b*-PCL nucleation and crystallization sequence, and for the first time, casting PEO-*b*-PCL films from toluene induced nucleation of PEO before nucleation of PCL.

The ATR-FTIR results demonstrated that the crystallization order was controlled by the interaction of the individual blocks with the solvent during casting. It was assumed that since crystallization order was different when drying from toluene, that the ATR crystal surface did not influence the crystallization process by preferentially nucleating one block over the other. In addition, given that the PEO and PCL were covalently linked, the individual block domain spacing was too small to be preferentially probed; thus, both components are irradiated simultaneously even if there is selective adsorption to the ATR crystal surface. If the ATR crystal induced nucleation, the same block component would likely be identified as crystallizing first in every trial. For chloroform and acetone, the PCL block preferred to phase separate, and the PEO stayed solvated longer during drying. This allows the PCL to crystallize first, as has been observed from the melt for symmetric PEO-*b*-PCL copolymers. Conversely, as the toluene solution was drying, the PEO phase separated first, and the PCL remained solvated, leading to PEO crystallization first. The solubility parameter for toluene [δ = 8.9 $(cal/cm^3)^{1/2}$] is further from that of PEO [δ = 10.0 $(cal/cm^3)^{1/2}$] than PCL [δ = 9.7 $(cal/cm^3)^{1/2}$]; whereas, the chloroform [δ = 9.3 $(cal/cm^3)^{1/2}$] and acetone [δ = 9.8 $(cal/cm^3)^{1/2}$] solubility parameters are closer to both blocks.[62] We have observed PEO

crystallization first from chloroform on occasion, but not in a controlled way as of yet. δ = 9.3 $(cal/cm^3)^{1/2}$ may indicate a crossover value between PEO poor solvents and solvents that may be equally compatible for both blocks. As δ increases, PCL should become more soluble, and above δ = 9.8 $(cal/cm^3)^{1/2}$, PEO becomes more soluble. It is important to note here that previous literature discussions label symmetric and asymmetric blocks based on molecular weight, and this convention was used here. However, in describing solvent-polymer interactions, the number of monomers in each block were not equal. PEO has a degree of polymerization of ~227, while PCL has a degree of polymerization of ~90. Using the amorphous densities, the monomer volumes are 0.066 nm^3 and 0.174 nm^3, respectively. The solvation of each block likely was not symmetric based on this analysis. In generalizing the crossover value, it is important to assess the molecular weight of each block as well as the relative block sizes. From a crystallization approach, the symmetric block copolymer (based on molecular weight) was used to ensure that coincident crystallization should occur to minimize crystallization preference based on molecular weight. For future solvation/precipitation analyses, the chain dimensions may be more appropriate; therefore, the reported crossover δ and crystallization order induced by different solvents may be sample dependent. It is unclear for the toluene solution whether small PEO crystals nucleated in solution, prior non-crystalline assembly occurred in solution (similar to micelle formation), or nucleation took place in a slightly solvated film. Each of these promotes PEO crystallization first in toluene. The ATR-FTIR spectrum indicates that the amount of toluene on the ATR crystal was similar to the amount of polymer (band at ~730 cm^{-1} from the dashed line for toluene in Figure 2a), which should represent a mostly dry film. These results are not conclusive for the mechanism of PEO nucleation and will be investigated further.

Slightly Soluble Solutions. To further prove that crystallization order could be controlled in symmetric PEO-*b*-PCL, *s*olvents able to achieve single crystal formation *via* solution crystallization (ethyl acetate, ethyl formate and methyl ethyl ketone) were precipitated to obtain single crystals of either PEO or PCL. Acetone, chloroform and toluene solutions could not be precipitated without extensive cooling; however, these secondary solutions formed precipitates slightly below room temperature. Single crystal formation in solution is a more definitive approach to show crystallization order as other factors such as substrate or evaporation effects are removed. As one block becomes less soluble during cooling, it should nucleate first and dictate the crystalline shape. Figure 3 shows the results of the solution crystallization for ethyl acetate and ethyl formate. Results from the methyl ethyl ketone (MEK) were less conclusive as it was difficult to obtain single crystals due to rapid precipitation, though it did appear that the crystals that formed had truncated-lozenge-like morphologies. Ethyl acetate and ethyl formate, however, both produced single crystals that were able to be concluded as PEO and PCL, respectively. The shapes of the single crystals and their identities were based off of the work done by Van Horn *et al.*[51] It appears that solutions of 10k-10.3k PEO-*b*-PCL in ethyl acetate formed PEO square single crystals (Figure 3a) and solutions from ethyl formate formed truncated-lozenge, or hexagonal, PCL single crystals (Figure 3b). The formation of these single crystals in ethyl acetate and ethyl formate suggests that the sequence of crystallization was controlled by solvent interactions. Specifically, PEO crystallized first in ethyl acetate and PCL crystallized first in ethyl formate. This information further proves the solvent effects on symmetric PEO-*b*-PCL copolymers and allows for the possibility of predicting crystallization order. For these solvents, both solution crystallization and crystallization during drying were used to identify the crystallization order to ensure that there were no concentration effects on the order.

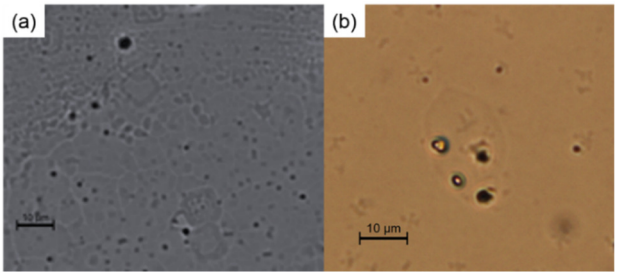


Figure 3. Optical microscopy images of single crystals of 10k-10.3k PEO-*b*-PCL (a) square-shaped PEO crystals grown in ethyl acetate and (b) truncated-lozenge PCL crystal grown in ethyl formate.

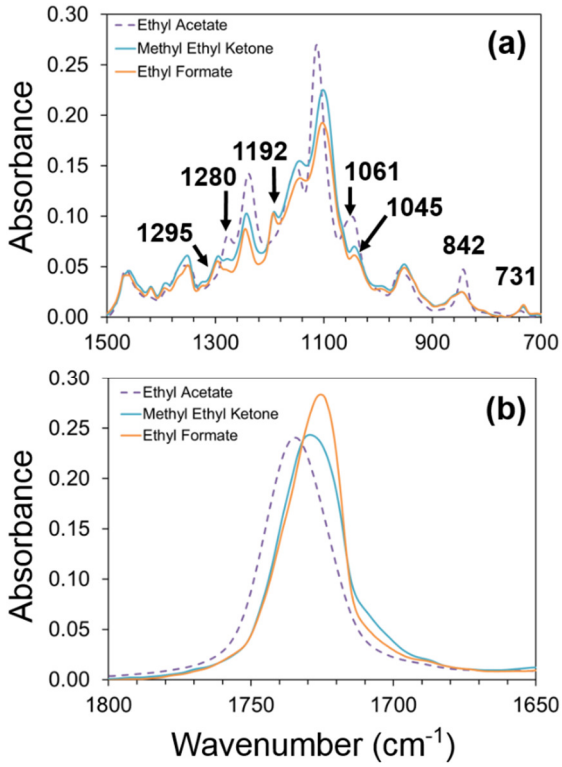


Figure 4. Overlayed ATR-FTIR spectra of 10k-10.3k PEO-*b*-PCL samples from ethyl acetate (dashed purple line), MEK (light blue line), and ethyl formate (orange line). The spectra range from 600 to 1500 cm^{-1} (a) and 1650 to 1800 cm^{-1} (b). The dashed line represents spectra in which PEO has crystallized first during drying.

Figure 4 shows the ATR-FTIR spectra of 10k-10.3k PEO-*b*-PCL thin films cast from ethyl acetate, ethyl formate, and MEK during drying. Only the spectra in which crystallization first was noted is presented. Just as Figure 2, the dashed line represents PEO crystallizing first in sequence, the solid lines represented PCL first, and all data was normalized by the ~1700 cm^{-1} bands. The same set of bands was used to identify crystallization as was discussed for

Figure 2. When ethyl formate (orange line) or MEK (light blue line) were used as the casting solvent, the solid line spectra showed growth of the PCL bands in the 600 – 1500 cm^{-1} range and the beginning of the shift of the 1734 cm^{-1} band to 1725 cm^{-1} before any PEO bands appeared. This suggests that in these two solvents, PCL separated from the solvent first and, therefore, crystallized first. For ethyl acetate (dashed purple line), the PEO bands appeared before any of the PCL bands. This indicated that the PEO crystallized first during drying. It should be noted here that when PEO crystallized first, the development of the 842 cm^{-1} band is much larger (or faster) at early stages of crystallization compared to those solvents where PCL crystallized first. This was also true for the toluene solution. It has been shown that the crystallization rate of PEO is much faster than PCL in symmetric block copolymers.[30] This phenomenon also applies to our system, though there may be some residual solvent that inhibits nucleation in the PCL block as noted by some distortions in the PEO bands where ethyl acetate bands overlap (1060 and 1240 cm^{-1} from Figure S1). In the case where PEO nucleated and grew first, the development of the crystalline morphology should be quite different than instances where PCL nucleated and grew first due to this difference in growth rates. The unique ability to nucleate PEO crystals first may lead to a new set of film properties for PEO-*b*-PCL copolymers where the block lengths are similar. In addition, the metastability of these crystals may be influenced by this switch in crystal formation sequence.

Predicting the crystallization properties of crystalline-crystalline polymer films is advantageous. The obvious correlation between crystallization order and solvent is the relative solubility parameters. To compare, the solubility parameters of all solvents (with some additional not discussed in detail) were collected and are listed in Table 2.[62] Again, the polymer solubility parameters are δ_{PEO} = 10.0 $(cal/cm^3)^{1/2}$ and δ_{PCL} = 9.7 $(cal/cm^3)^{1/2}$. As demonstrated for the “common solvent” solutions, the relative value of the solubility

parameter helps predict which block prefers to remain solvated during drying. A similar trend is seen for the “slightly soluble” solvents. There is a range of solubility parameters where the solvation of each block is more competitive (δ = 9.29 – 9.82 $(cal/cm^3)^{1/2}$ in Table 2). Thus, the solution storage and casting temperatures (and possibly humidity) must be maintained to prevent solution crystallization and precipitation prior to or during drying. Here, the two blocks may be equally compatible with the solvent, and the crystallization process would be driven by thermodynamics similar to the melt. This is a little counter-intuitive since the PCL block should be more soluble in this range. It is also plausible that the change in the Flory-Huggins interaction parameter, χ, for the solvent-polymer block interaction has a different dependence on temperature for each block.[39] This could mean that the ability to switch the crystallization order is possible for one solvent. Further investigation is needed to confirm this. The vapor pressure, or evaporation rate, of the solvent is influential as the rate of nucleation compared to the rate of evaporation where each block’s time solvated influences the crystallization order, too. Therefore, this information was provided in Table 2 for comparison. For all solvents, the solubility of homopolymer 10.2k PEO and 9.5k PCL was evaluated to support the drying experiments. 1% solutions were made (and heated when necessary) to dissolve the homopolymer powder. In all cases, the homopolymer that was insoluble when cooled back to room temperature matched the one that crystallized first during drying. The only exceptions were chloroform and MEK, where both homopolymers were soluble in chloroform and both were insoluble in MEK at room temperature. This also confirms that the solubility of the PEO-*b*-PCL copolymer in different solvents is enhanced by the more soluble block.

Table 2. Solvent Characteristics and Crystallization Order

Solvent	Solubility Parameter ($[cal/cm^3]^{1/2}$)	Vapor Pressure (kPa)	Crystallization Order
Diethyl Ether[a]	*7.72*	*71.7*	*PEO First*
Amyl Acetate[a]	*8.41*	*0.6*	*PEO First*
Toluene	8.9	3.79	PEO First
Ethyl Acetate	8.9	12.6	PEO First
Methyl Ethyl Ketone	9.29	12.6	PCL First[b]
Chloroform	9.29	26.2	PCL First[b]
Ethyl Formate	9.58	32.3	PCL First[b]
Acetone	9.82	30.8	PCL First[b]
Dichloromethane	9.92	58.2	PCL First
n-Hexanol[a]	*10.7*	*0.11*	*PCL First*
Ethanol[a]	*12.92*	*7.87*	*PCL First*

[a]insoluble at room temperature, solution crystallization during cooling

[b]crystallization order and solubility are more sensitive to temperature

Film Morphology. Films were prepared from 1% solutions of 10k-10.3k PEO-*b*-PCL in each solvent and analyzed using polarized optical microscopy (POM) and transmission FTIR to evaluate the influence of solvent and crystallization order on the final structure. Figure 5 shows POM images of as-cast films made from each of the six solvents. The use of a quarter-wave plate imparted the color which enhances the morphological observations. The left side of Figure 5 shows the films dried from acetone (5a) and ethyl formate (5d), where, according to ATR-FTIR data, PCL nucleation occurred first. The middle images are from chloroform (5b) and MEK (5e). Again, PCL nucleation occurred first, but the solubility parameters indicated that the nucleation process may be more competitive, i.e. under certain conditions it may be possible for PEO to nucleate first. Finally, the images on the right side represent films dried from toluene (5c) and ethyl acetate (5f), where PEO nucleated first. Figure S3 in the Supporting Information shows POM images of films made from homopolymer PCL and homopolymer PEO for comparison. These images help support

conclusions based on the crystallization order since the block crystallizing first should control development of crystal morphology as observed by POM.

In all films except acetone (Figure 5a) and toluene (Figure 5c), a polycrystalline morphology was observed. Figures 5a and 5c seem to demonstrate that crystallization began in solution as a precipitate due to the appearance of aggregates. Full solution crystallization did not occur, and continuous films were made after drying. It is unclear, then, how the aggregates observed in Figures 5a and 5c were developed. It should be noted that these two solvents were near the crossover between film crystallization and solution crystallization as noted in Table 2. Although the solutions were homogeneous at room temperature, during drying, the polymer concentration increased in solution, so it was not unexpected that precipitation may begin to occur prior to complete drying. According to the ATR-FTIR data, PCL crystals should be the dominant component in Figure 5a, and PEO crystals should be the dominant component in Figure 5c. These morphological observations are supported by the POM images in Figure S3, where it was observed that the PCL homopolymer showed aggregation from acetone and that PEO homopolymer aggregated from toluene. Figure 5a shows some birefringence due to the appearance of yellow and blue streaks within the aggregates. It was inferred that these are edge-on crystals, though the morphology is not spherulitic in nature. The observed morphology in Figure 5c lacks any birefringence. The only distinguishing feature is the small aggregates. However, the ATR-FTIR data confirmed that crystallization occurred in films dried from toluene. One explanation is that the crystals have adopted a flat-on morphology instead of the typical edge-on (spherulitic crystals). If the crystals were flat-on, no birefringence is observed. Transmission FTIR analysis was done to confirm both the presence of crystals and to support the presence of flat-on crystals and is discussed in a subsequent section.

Figures 5b and 5e are most representative of the POM morphology expected when PCL nucleated first. These have a more regular Maltese cross pattern, typical of polymer spherulites, and a higher nucleation density (smaller crystallite sizes). Because the films were thick and the nucleation density was high, it was difficult to observe the outline of the polycrystalline spherulite. Also, the chloroform film (Figure 5b) had a brighter birefringence compared to the MEK film (Figure 5e). The cause is unclear, though it may be due to less PEO crystallization in the MEK film, which is supported in the transmission FTIR discussion below. These morphologies were most similar to the homopolymer PCL POM images in Figure S3.

Figure 5d shows the polycrystalline morphologies when dried from ethyl formate solution. Here, there were two distinguishable crystal morphologies: a small, densely packed spherulitic crystal, similar to the PCL morphologies, and two larger spherulites with easily identifiable lamellae. These second crystal structures are representative of PEO crystals (see Figure S3 for examples). This indicates that the nucleation order for each block was more competitive during drying. Here, PCL nucleated first in most areas; however, there were a few localized spots where PEO nucleated first. In fact, it appeared that the PCL crystals were dispersed among the growing PEO spherulite. This is likely a manifestation of crystallization in three dimensions. The ATR-FTIR data showed that PCL nucleated first from ethyl formate. This is supported in the POM image by the larger density of PCL spherulites. Spectra taken after the first identification of crystalline bands showed that PEO crystallized nearly simultaneously with PCL, which supports the possibility of localized PEO nucleation before PCL nucleation. For samples with symmetric molecular weights, coincident crystallization has a competitive nucleation process at large undercoolings, but the ability to observe

morphological evidence is dependent on the growth rates of the spherulites. The appearance of both spherulitic morphologies has been observed in these symmetric samples.[46]

The spherultes grown from ethyl acetate (Figure 5f) had a larger radial size and more distinct lamellar features compared to those where PCL crystallized first. This morphology was indicative of PEO nucleation and growth prior to PCL nucleation, similar to the two spherulites in Figure 5d. For clarity, the homopolymer POM images in Figure S3 exemplify this conclusion. The ethyl acetate film shows spherulitic crystals with a different birefringence than those in the PCL-first films. The birefringence is not as well defined, which is characteristic of some PEO crystallization.[62] Because PEO crystal growth is faster than PCL,[30] there is no evidence of PCL crystals even when the nucleation density was small, unlike the PCL-dominated morphologies. This crystal morphology supported the ATR-FTIR observation that PEO crystallizes first from ethyl acetate.

Overall, the morphological results in Figure 5 show that the larger scale assembly of the polymer crystals was influenced by the crystallization order, which should impart new properties on these materials. It is unclear whether the observed differences were caused by polymer pre-assembly in solution, competition between solvent-polymer and substrate-polymer interactions, or simply solvent retention in the block with preferential solvent-polymer interactions. The mechanism for nucleation and crystal morphologies is under further investigation.

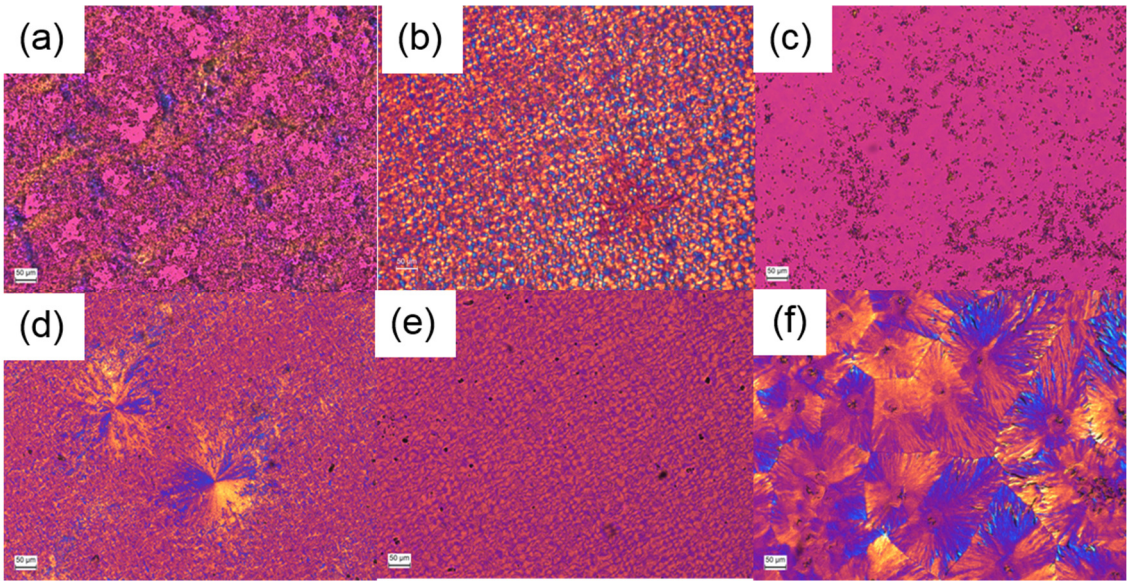


Figure 5. POM images of 10k-10.3k PEO-*b*-PCL films prepared from various solvents: (a) acetone, (b) chloroform, (c) toluene, (d) ethyl formate, (e) methyl ethyl ketone, and (f) ethyl acetate. The scale bar represents 50 μm.

Transmission FTIR analysis was performed on the as-cast films to confirm crystallization of both the PEO and PCL blocks, as it was not obvious from POM images, except for ethyl formate, and to identify crystal lamellar orientation to compare with POM images. Figure 6 shows the spectra for films dried from each solvent (colors correspond to those used previously). In Figure 6a, strong bands at 731 cm^{-1} and 842 cm^{-1} were evidence that both blocks crystallized in all films. Since these bands are directly correlated to the crystalline portion of the block domain, the relative heights provide insight to the crystallinity of each block (direct calculation is difficult since the molar absorptivities are unknown). It also should be noted that DSC analysis of melting curves is difficult for samples where coincident crystallization occurs. There is significant overlap in melting peaks, and the melting mechanism is not well-known. Therefore, analysis of the ΔH_m for each block is complicated.[1,25,28,33,40,45-47] In the transmission FTIR set-up, a crude quantitative comparison was applied to provide insight into the consequences of switching crystallization order. While the 731 cm^{-1} PCL band is nearly equal for all solvents, except ethyl formate, the height of the

842 cm^{-1} band indicates the amount of PEO crystallization. From Figure 6a, it appears that PEO crystallization is highest when films are made from ethyl acetate (purple line) and toluene (red line) and lowest when crystallized from MEK (light blue line). This trend further supports that PEO crystallized first from ethyl acetate and toluene, which allowed the PEO crystallinity to be maximized prior to and during PCL crystallization. Conversely, the PEO crystallinity should be lower in films where PCL crystallized first.

In Figure 6b, the spectra for all films in the range of 1000 cm^{-1} to 1500 cm^{-1} is shown. Absorption bands in this range have polarizations associated with the chain axis direction and should indicate crystal orientation in the film. As listed in Table 1, the polarization of some bands is parallel or perpendicular to the chain axis (or crystal *c*-axis). Because of this distinct polarization, it was possible to infer crystal orientation from the FTIR data to compare with POM images. For the crystal bands that have parallel polarization, the alignment in the IR beam determines the absorption of these bands. The ones of interest are indicated with arrows in Figure 6b. They are 1192 and 1295 cm^{-1} for PCL crystals and 1343 cm^{-1} for PEO crystals.[52-54] For films dried from toluene, these bands are significantly lower than those in other films, while the bands at 1280 cm^{-1} (PEO perpendicular) and 1490 cm^{-1} (overlap of PCL and PEO perpendicular) are comparable for all solvents. It should be noted that others bands not identified have parallel polarization as well. Only a few bands were chosen as examples. When the vibrations parallel to the crystal chain axis are parallel to the IR beam, the propagating IR wave does not interact with them. Thus, a decrease in the designated band absorption is evidence of crystal orientation, namely, flat-on crystals, where the crystal's normal vector is perpendicular to the substrate. In the edge-on conformation, the parallel vibrations are perpendicular to the IR beam; therefore, the absorption at 1192, 1295, and 1343 cm^{-1} was much larger in all other solvents compared to toluene. It should be noted that

for both flat-on and edge-on orientations, both block's crystals have the same orientation. In other words, the PCL crystals' *c*-axes and PEO crystals' *c*-axes are aligned in the same direction. This analysis was not realistic for the ATR-FTIR data since the IR beam was at an angle when penetrating the film surface.

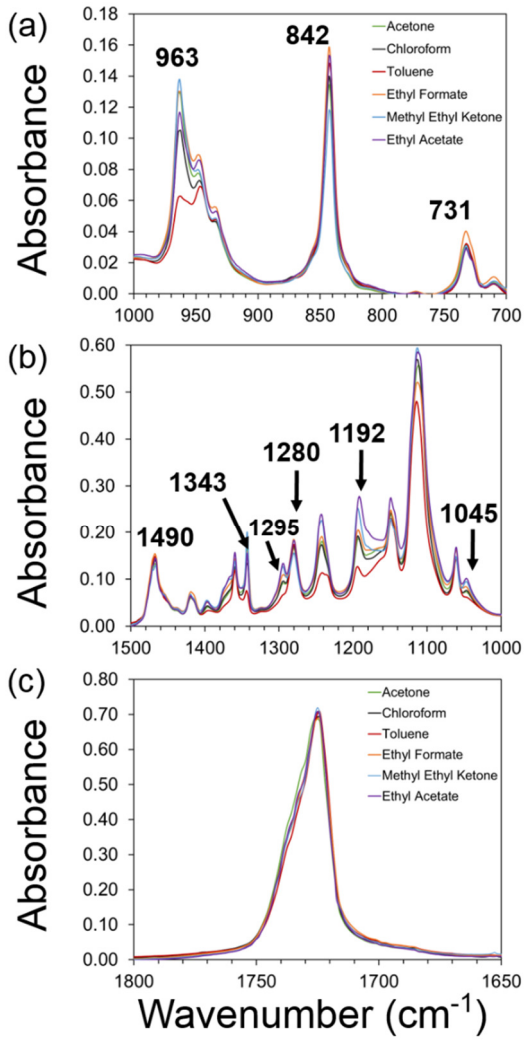


Figure 6. Transmission FTIR spectra of 10k-10.3k PEO-*b*-PCL films prepared from different solvents: (a) 700 – 1000 cm^{-1}, (b) 1000 – 1500 cm^{-1}, and (c) 1675 – 1775 cm^{-1}. The solvents are acetone (green line), chloroform (black line), toluene (red line), ethyl formate (orange line), MEK (blue line), and ethyl acetate (purple line).

In Figure 6c, the FTIR spectra are shown for the PCL carbonyl band around 1700 cm^{-1}. Again, all spectra were normalized by the total area of these bands taking into account the

amorphous and crystalline PCL fractions. As was shown by the 731 cm^{-1} band in Figure 6a, the measure of crystallinity (area of the 1725 cm^{-1} band as a fraction of the total area) appears to be similar for all samples. The acetone film (green line) appeared to have a little more amorphous fraction (band absorbance at 1734 cm^{-1}), and the toluene film (red line) appeared to have a little less, though neither of these samples was drastically different than the others. If these results are taken to be significant, it would imply that the crystallization from acetone may be less perfect due to fast evaporation and that the flat-on orientation in the toluene film provided the space to increase crystallinity since growth was two dimensional, parallel to the substrate, instead of the typical three-dimensional spherulitic growth.[64]

With the morphological evidence from the POM image in Figure 5c and the FTIR spectra of Figure 6b, it was concluded that the toluene film has flat-on crystals with some aggregates. Perpendicular vibrational bands associated with crystallization were present in the toluene spectra; therefore, crystallization was confirmed though not obvious from the POM image. The acetone film's transmission FTIR spectra shows similar absorbances to the other films. This supported the fact that some, if not many, of the crystals grown from acetone have an edge-on orientation even with the appearance of aggregates. From the FTIR data, the crystal orientation should be flat-on due to the diminished bands at 1192, 1295, and 1343 cm^{-1}. The POM image in Figure 5c shows some aggregate crystals but the dominant crystal orientation must be flat-on because of the lack of absorbance at the noted wavenumbers. These two observations indicate that the bulk of the PEO-*b*-PCL film dried from toluene had significant crystallization with a majority flat-on orientation and some aggregates on the surface that are visible in the POM image.

Crystallization from the Melt. In order to demonstrate that the crystallization sequence was driven by solvent interactions, a film dried from toluene was melted and recrystallized. It was assumed that after melting, PCL would crystallize first, as has been observed by numerous other studies.[25,30,58-61] However, it was found that only after multiple melts, the PCL block crystallized first regardless of block crystallization sequence during drying. Using ATR-FTIR analysis of the dried toluene solution film, the sample was heated above the melting temperature of both blocks and held for a few minutes at that temperature with subsequent air cooling back to room temperature. The collected spectra are shown in Figure 7. The blue line in Figure 7 is the film after drying from toluene. The black line is the melt spectra. The dashed purple line is cooling after to two melt cycles, and the solid green line represents the crystallization process during cooling from the melt after three melt cycles. The dashed purple line shows that after two cycles, the PEO crystallized first during cooling (appearance of the 842, 1061, and 1280 cm^{-1} bands without any indication of PCL crystallization). This observation is interesting since it implies that the crystallization order may be preserved even after melting. Work is being done currently to investigate this further. In the solid green line spectrum (3rd cooling), the appearance of the 731, 1045, 1192, and 1295 cm^{-1} bands and a broadening of the 1700 cm^{-1} band, or increase in 1725 cm^{-1} band with a decrease in the 1734 cm^{-1} band, during the third cooling proves PCL crystallized before any band that would indicate PEO was crystallized. This was further evidence that the ATR-FTIR probing method does not preferentially identify the crystallization of one block over the other since during drying and during cooling each block was identified as crystallizing first under different conditions. Several melts were needed possibly to ensure that solvent was removed completely and that the melt became as homogeneous as possible. It is unclear whether the crystallization of PEO prior to PCL from the first two melt-cooling cycles is due to residual

solvent or a type of memory effect where the local chains, while melted, may nucleate more easily, similar to a self-seeding approach. From this, it was determined that PCL preferred to crystallize first sequentially in the 10k-10.3k PEO-*b*-PCL copolymer after solvent effects were removed, as has been reported previously for other symmetric copolymers. Additionally, this further proves that the solvent primarily affected the crystallization sequence for these crystalline-crystalline diblock copolymer films, similar to solution crystallization.

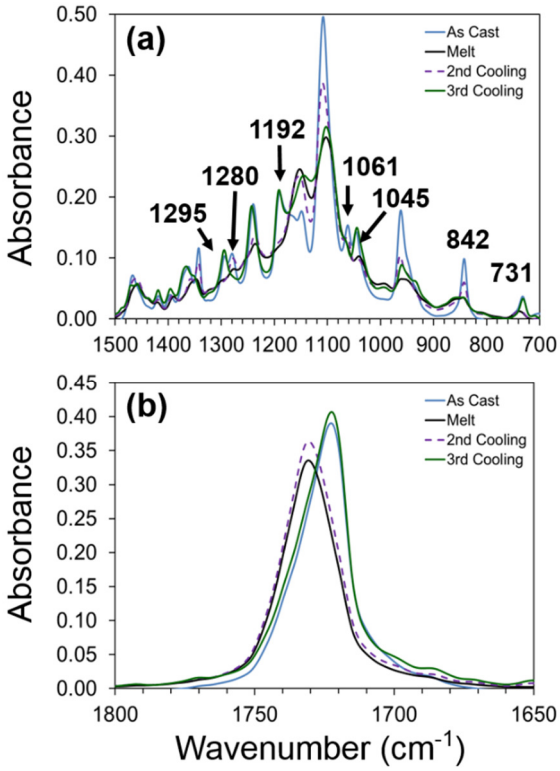


Figure 7. Overlayed ATR-FTIR spectra of a 10k-10.3k PEO-*b*-PCL sample cast from toluene. The sample was melted and cooled over three cycles. Data is shown for the film: as cast (blue line), the melt (black line), during the second cooling (dashed purple line), and during the third cooling (green line). The spectra range from 700 to 1500 cm^{-1} (a) and1650 to 1800 cm^{-1} (b). The dashed line represents spectra in which PEO has crystallized first during cooling.

These results for the crystallization of 10k-10.3k PEO-*b*-PCL demonstrate for the first time that the crystallization order in crystalline-crystalline block copolymer films can be controlled using different casting solvents. We have observed similar results in a 5k-5k PEO-*b*-PCL copolymer; however, it was less pronounced due to the enhanced solubility of lower

molecular weight polymers. As such, the effects of this methodology are likely molecular weight dependent. Current work is focused on the consequences of this reversed crystallization sequence. For example, the crystallization kinetics, crystal morphology, and crystal metastability or resulting melting temperatures of the as-crystallized lamellae will be compared to those where PCL crystallized first. The connection between solvent-polymer interactions, crystallization order, and morphological development are unclear.[35-36] The range of PCL weight fractions where the crystallization order switch occurs is also under investigation. In addition, this phenomenon may affect crystallization in crystalline-crystalline copolymers where T_m's are different but within a range where solvent interactions may influence crystallization order or overall crystallinity. This should greatly change the thermodynamic metastability of these crystals. The control of crystallization order should lead to enhanced properties and more diverse applications of PEO-*b*-PCL and other crystalline-crystalline block copolymers.

SUMMARY

Solvent interactions were utilized successfully in order to force a change in crystallization sequence in the symmetric diblock copolymer 10k-10.3k PEO-*b*-PCL. ATR-FTIR and solution crystallization analyses of PEO-*b*-PCL crystallization revealed that toluene and ethyl acetate promoted PEO nucleation to occur first, suggesting that these solvents do not interact favorably with PEO. Acetone, chloroform, ethyl formate, and methyl ethyl ketone all showed nucleation of PCL first, meaning solvent-PCL interactions are less favorable or that solvent-block interactions are nearly equal. Moreover, it was found that once solvent effects are diminished *via* melting, PCL always crystallized first, further proving that solvent affected the crystallization of PEO-*b*-PCL. The relationship between the solubility parameter of the solvent and each constituent polymer block is a good predictor for crystallization order as well as

whether solution crystallization (or precipitation) or film crystallization during drying occurs. This research is important to broaden the available properties and applications of PEO-*b*-PCL and other CC copolymers.

SUPPORTING INFORMATION

The Supporting Information is available free of charge on the ACS Publications website.

ATR-FTIR data showing the spectra for pure solvents, homopolymer PEO and PCL, spectra showing the drying process for ethyl acetate and MEK, and POM images for homopolymer PEO and PCL films cast from all solvents

AUTHOR INFORMATION

Corresponding Author

*Email: rvanhorn@allegheny.edu

Author Contributions

The manuscript was written through contributions of all authors. All authors have given approval to the final version of the manuscript. N.B. performed a majority of the research and prepared the manuscript with help from R.M.V.H. All other authors contributed in the development of appropriate solvents and experimental procedures.

Funding Sources

NSF DMR-1606532

ACKNOWLEDGMENT

The authors would like to thank the National Science Foundation (DMR-1606532) for funding for this project.

REFERENCES

1. Castillo, R. V.; Müller, A. J. Crystallization and Morphology of Biodegradable or Biostable Single and Double Crystalline Block Copolymers. *Prog. Polym. Sci.* **2009**, *34*, 516.
2. He, W.-N.; Xu, J.-T. Crystallization Assisted Self-assembly of Semicrystalline Block Copolymers. *Prog. Polym. Sci.* **2012**, *37*, 1350-1400.
3. Hamley, I. W.; Castelletto, V.; Castillo, R. V.; Müller, A. J.; Martin, C. M.; Pollet, E.; Dubois, P. Crystallization in Poly(l-lactide)-*b*-poly(ε-caprolactone) Double Crystalline

Diblock Copolymers: A Study Using X-ray Scattering, Differential Scanning Calorimetry, and Polarized Optical Microscopy. *Macromolecules* **2005***, 38*, 463-472.
4. Castillo, R. V.; Müller, A. J.; Raquez, J.; Dubois, P. Crystallization Kinetics and Morphology of Biodegradable Double Crystalline PLLA-*b*-PCL Diblock Copolymers. *Macromolecules* **2010***, 43*, 4149-4160.
5. Zhu, L.; Cheng, S. Z. D.; Calhoun, B. H.; Ge, Q.; Quirk, R. P.; Thomas, E. L.; Hsiao, B. S.; Yeh, F.; Lotz, B. Crystallization Temperature-Dependent Crystal Orientations within Nanoscale Confined Lamellae of a Self-Assembled Crystalline–Amorphous Diblock Copolymer. *J. Am. Chem. Soc.* **2000***, 122*, 5957-5967.
6. Hamley, I. W.; Fairclough, J. P. A.; Terrill, N. J.; Ryan, A. J.; Lipic, P. M.; Bates, F. S.; Towns-Andrews, E. Crystallization in Oriented Semicrystalline Diblock Copolymers. *Macromolecules* **1996***, 29*, 8835-8843.
7. Wang, J.; Dong, C. Synthesis, Sequential Crystallization and Morphological Evolution of Well-Defined Star-Shaped Poly(ε-caprolactone)-*b*-poly(L-lactide) Block Copolymer. *Macromol. Chem. Phys.* **2006***, 207*, 554-562
8. Lin, M.; Chen, H.; Su, W.; Su, C.; Jeng, U.; Tzeng, F.; Wu, J.; Tsai, J.; Hashimoto, T. Interactive Crystallization Kinetics in Double-Crystalline Block Copolymer. *Macromolecules* **2012***, 45*, 5114-5127.
9. Nojima, S.; Kiji, T.; Ohguma, Y. Characteristic Melting Behavior of Double Crystalline Poly(ε-caprolactone)-*block*-polyethylene Copolymers. *Macromolecules* **2007***, 40*, 7566-7572.
10. Nojima, S.; Akutsu, Y.; Washino, A.; Tanimoto, S. Morphology of Melt-quenched Poly(ε-caprolactone)-*block*-polyethylene Copolymers. *Polymer* **2004***, 45*, 7317-7324.
11. Sun, L.; Liu, Y.; Zhu, L.; Hsiao, B. S.; Avila-Orta, C. A. Self-assembly and Crystallization Behavior of a Double-Crystalline Polyethylene-*block*-Poly(ethylene oxide) Diblock copolymer. *Polymer* **2004***, 45*, 8181-8193.
12. Li, S.; Myers, S. B.; Register, R. A. Solid-State Structure and Crystallization in Double-Crystalline Diblock Copolymers of Linear Polyethylene and Hydrogenated Polynorbornene. *Macromolecules* **2011***, 44*, 8835-8844.
13. Myers, S. B.; Register, R. A. Crystalline−Crystalline Diblock Copolymers of Linear Polyethylene and Hydrogenated Polynorbornene. *Macromolecules* **2008***, 41*, 6773-6779.
14. Castillo, R. V.; Müller, A. J.; Lin, M.; Chen, H.; Jeng, U.; Hillmyer, M. A. Confined Crystallization and Morphology of Melt Segregated PLLA-b-PE and PLDA-*b*-PE Diblock Copolymers. *Macromolecules* **2008***, 41*, 6154-6164.
15. Nojima, S.; Ito, K.; Ikeda, H. Composition Dependence of Crystallized Lamellar Morphology Formed in Crystalline–Crystalline Diblock Copolymers. *Polymer* **2007***, 48*, 3607-3611.
16. Hamley, I. W.; Parras, P.; Castelletto, V.; Castillo, R. V.; Müller, A. J.; Pollet, E.; Dubois, P.; Martin, C. M. Melt Structure and its Transformation by Sequential Crystallization of the Two Blocks within Poly(L-lactide)-*block*-Poly(ε-caprolactone) Double Crystalline Diblock Copolymers. *Macromol. Chem. Phys.* **2006***, 207*, 941-953.
17. Li, L.; Meng, F.; Zhong, Z.; Byelov, D.; de Jeu, W. H.; Feijen, J. Morphology of a Highly Asymmetric Double Crystallizable Poly(epsilon-caprolactone-*b*-ethylene oxide) Block Copolymer. *J Chem Phys* **2007***, 126*, 024904.
18. Burbidge, P. G. Theory of Microphase Separation in Block Copolymers; Cambridge; University Press: Cambridge, **1952**; Vol. 4., pp 1602-1617.

19. Khokhlov, A. R.; Khalatur, P. G. Microphase Separation in Diblock Copolymers with Amphiphilic Block: Local Chemical Structure Can Dictate Global Morphology. *Chem. Phys. Lett.* **2008***, 461*, 58-63.
20. Lohse, D. J.; Hadjichristidis, N. Microphase separation in block copolymers. *Current Opinion in Colloid & Interface Science* **1997***, 2*, 171-176.
21. Nojima, S.; Fukagawa, Y.; Ikeda, H. Interactive Crystallization of a Strongly Segregated Double Crystalline Block Copolymer with Close Crystallizable Temperatures. Macromolecules 2009, 42, 9515-9522.
22. Xue, F.; Jiang, S. Crystallization Behaviors and Structure Transitions of Biocompatible and Biodegradable Diblock Copolymers. *Polymers* **2014***, 6*, 2116-2145.
23. Quiram, D. J.; Register, R. A.; Marchand, G. R.; Ryan, A. J. Dynamics of Structure Formation and Crystallization in Asymmetric Diblock Copolymers. *Macromolecules* **1997***, 30*, 8338-8343.
24. Rangarajan, P.; Register, R.A.; Fetters, L.J.; Bras, W.; Naylor, S.; Ryan, A.J. Crystallization of a Weakly Segregated Polyolefin Diblock Copolymer. *Macromolecules* **1995***, 28*, 4932-4938.
25. Arnal, M. L.; López-Carrasquero, F.; Laredo, E.; Müller, A. J. Coincident or Sequential Crystallization of PCL and PEO Blocks within Polystyrene-*b*-poly(ethylene oxide)-*b*-poly(ε-caprolactone) Linear Triblock Copolymers. *Eur. Polym. J.* **2004***, 40*, 1461-1476.
26. Nojima, S.; Fukagawa, Y.; Ikeda, H. Interactive Crystallization of a Strongly Segregated Double Crystalline Block Copolymer with Close Crystallizable Temperatures. *Macromolecules* **2009***, 42*, 9515-9522.
27. Müller, A. J.; Albuerne, J.; Marquez, L.; Raquez, J.; Degée, P.; Dubois, P.; Hobbs, J.; Hamley, I. W. Self-nucleation and Crystallization Kinetics of Double Crystalline Poly(p-dioxanone)-*b*-poly(ε-caprolactone) Diblock Copolymers. *Faraday Discuss.* **2005***, 128*, 231-252.
28. Müller, A. J.; Albuerne, J.; Esteves, L. M.; Marquez, L.; Raquez, J.; Degée, P.; Dubois, P.; Collins, S.; Hamley, I. W. Confinement Effects on the Crystallization Kinetics and Self-Nucleation of Double Crystalline Poly(p-dioxanone)-*b*-poly(ε-caprolactone) Diblock Copolymers. *Macromol. Symp.* **2004***, 215*, 369-382.
29. Albuerne, J.; Márquez, L.; Müller, A. J.; Raquez, J. M.; Degée, P.; Dubois, P.; Castelletto, V.; Hamley, I. W. Nucleation and Crystallization in Double Crystalline Poly(p-dioxanone)-*b*-poly(ε-caprolactone) Diblock Copolymers. *Macromolecules* **2003***, 36*, 1633-1644.
30. (a) He, C.; Sun, J.; Zhao, T.; Chen, X.; Jing, X. Formation of a Unique Crystal Morphology for the Poly(ethylene glycol)–Poly(ε-caprolactone) Diblock Copolymer *Biomacromolecules* **2006**, *7*, 252-258. (b) He, C.; Sun, J.; Ma, J.; Chen, X.; Jing, X. Composition Dependence of the Crystallization Behavior and Morphology of the Poly(ethylene oxide)-poly(ε-caprolactone) Diblock Copolymer. *Biomacromolecules* **2006**, *7*, 3482-3489.
31. Huang, S.; Jiang, S.; An, L.; Chen, X. Crystallization and Morphology of Poly(ethylene oxide-*b*-lactide) Crystalline–Crystalline Diblock Copolymers. *J. Polym. Sci. B Polym. Phys.* **2008**, *46*, 1400-1411.
32. Du, Z.; Xu, J.; Fan, A. Regulation of Micellar Morphology of PCL-*b*-PEO Block Copolymers by Crystallization Temperature. *Macromolecules* **2008**, *29*, 467-471.

33. Chiang, Y.; Hu, Y.; Li, J.; Huang, S.; Kuo, S. Trilayered Single Crystals with Epitaxial Growth in Poly(ethylene oxide)-*block*-poly(ε-caprolactone)-*block*-poly(l-lactide) Thin Films. *Macromolecules* **2015**, *48*, 8526-8533.
34. Graham, N. B.; Nwachuku, N. E.; Walsh, D. J. Interaction of Poly(ethylene oxide) with Solvents: Preparation and Swelling of a Crosslinked Poly(ethylene oxide) Hydrogel. *Polymer* **1982**, *23*, 1345-1349.
35. Sasaki, T.; Miyazaki, A.; Sugiura, S.; Okada, K. Crystallization of Poly(ethylene oxide) from Solutions of Different Solvents. *Polym. J.* **2002**, *34*, 794-800.
36. Toolan, D. T. W.; Isakova, A.; Hodgkinson, R.; Reeves-McLaren, N.; Hammond, O.S.; Edler, K. J.; Briscoe, W. H.; Arnold, T.; Gough, T.; Topham, P. D.; Howse, J. R. Insights into the Influence of Solvent Polarity on the Crystallization of Poly(ethylene oxide) Spin-Coated Thin Films via in Situ Grazing Incidence Wide-Angle X-ray Scattering. *Macromolecules*, **2016**, *49*, 4579-4586.
37. Zheng, X.; Xu, Q.; He, L.; Yu, N.; Wang, S.; Chen, Z.; Fu, J. Modification of Graphene Oxide with Amphiphilic Double-Crystalline Block Copolymer Polyethylene-*b*-poly(ethylene oxide) with Assistance of Supercritical CO_2 and Its Further Functionalization. *J. Phys. Chem. B* **2011***, 115*, 5815-5826.
38. Handa, Y. P.; Zhang, Z.; Roovers, J. Compressed-gas-induced Crystallization in *tert*-Butyl Poly(ether ether ketone). *J. Polym. Sci. B Polym. Phys.* **2001***, 39*, 1505-1512.
39. Flory, P.J. *Principles of Polymer Chemistry*; Cornell University Press: Ithaca, NY, 1953.
40. Li, Y.; Zhou, J.; Zhang, J.; Gou, Q.; Gu, Q.; Wang, Z. Morphology of Poly(Ethylene Oxide)-*b*-Poly(ϵ-Caprolactone) Spherulites Formed Under Compressed CO_2. *J. Macromol. Sci., Part B* **2014***, 53*, 1137-1144.
41. Müller, A. J.; Arnal, M. L.; Balsamo, V. In *Crystallization in Block Copolymers with More than One Crystallizable Block;* Reiter, G., Strobl, G. R., Eds.; Progress in Understanding of Polymer Crystallization; Springer Berlin Heidelberg: 2007; pp 229-259.
42. Müller, A. J.; Castillo, R. V.; Hillmyer, M. Nucleation and Crystallization of PLDA-b-PE and PLLA-b-PE Diblock Copolymers. *Macromol. Symp.* **2006***, 242*, 174-181.
43. Albuerne, J.; Márquez, L.; Müller, A. J.; Raquez, J. M.; Degée, P.; Dubois, P.; Castelletto, V.; Hamley, I. W. Nucleation and Crystallization in Double Crystalline Poly(p-dioxanone)-b-poly(ε-caprolactone) Diblock Copolymers. *Macromolecules* **2003***, 36*, 1633-1644.
44. Li, L.; Meng, F.; Zhong, Z.; Byelov, D.; de Jeu, W. H.; Feijen, J. Morphology of a Highly Asymmetric Double Crystallizable Poly(epsilon-caprolactone-b-ethylene oxide) Block Copolymer. *J Chem Phys* **2007***, 126*, 024904.
45. Suzuki, Y.; Duran, H.; Steinhart, M.; Butt, H.; Floudas, G. Suppression of Poly(ethylene oxide) Crystallization in Diblock Copolymers of Poly(ethylene oxide)-b-poly(ε-caprolactone) Confined to Nanoporous Alumina. *Macromolecules* **2014***, 47*, 1793-1800.
46. Xu, Y.; He, Y.; Wei, J.; Fan, Z.; Li, S. Morphology and Melt Crystallization of PCL-PEG Diblock Copolymers. *Macromol. Chem. Phys.* **2008**, *209*, 1836-1844
47. Müller, A. J.; Arnal, M. L.; López-Carrasquero, F. Nucleation and crystallization of PS-b-PEO-b-PCL triblock copolymers. *Macromol. Symp.* **2002***, 183*, 199-204.

48. Meier, M. A. R.; Aerts, S. N. H.; Staal, B. B. P.; Rasa, M.; Schubert, U. S. PEO-*b*-PCL Block Copolymers: Synthesis, Detailed Characterization, and Selected Micellar Drug Encapsulation Behavior. *Macromol. Rapid Commun.* **2005***, 26*, 1918–1924.
49. Nagarajan, R.; Ganesh, K. Block Copolymer Self-assembly in Selective Solvents: Spherical Micelles with Segregated Cores. *J. Chem. Phys.* **1989***, 90*, 5843-5856.
50. Yu, Y.; Zhang, L.; Eisenberg, A. Morphogenic Effect of Solvent on Crew-Cut Aggregates of Amphiphilic Diblock Copolymers. *Macromolecules* **1998***, 31*, 1144-1154.
51. Van Horn, R. M.; Zheng, J. X.; Sun, H.; Hsiao, M.; Zhang, W.; Dong, X.; Xu, J.; Thomas, E. L.; Lotz, B.; Cheng, S. Z. D. Solution Crystallization Behavior of Crystalline–Crystalline Diblock Copolymers of Poly(ethylene oxide)-*block*-poly(ε-caprolactone). *Macromolecules* **2010***, 43*, 6113-6119.
52. Zheng, Y.; Bruening, M. L.; Baker, G. L. Crystallization of Polymer Brushes with Poly(ethylene oxide) Side Chains. *Macromolecules* **2007***, 40*, 8212-8219.
53. Keroack, D.; Zhao, Y.; Prud'homme, R. E. Molecular orientation in crystalline miscible blends. *Polymer* **1999***, 40*, 243-251.
54. Yan, C.; Li, H.; Zhang, J.; Ozaki, Y.; Shen, D.; Yan, D.; Shi, A.; Yan, S. Surface-Induced Anisotropic Chain Ordering of Polycarprolactone on Oriented Polyethylene Substrate: Epitaxy and Soft Epitaxy. *Macromolecules* **2006***, 39*, 8041-8048.
55. Lotz, B.; Kovacs, A. J. Properties of Polyoxyethylene-Polystyrene Diblock Copolymers: I. Preparation, Composition and Microscopic Study of Single Crystals. *Kolloid Z. Z. Polym.* **1966**, *209*, 97-114
56. Chen, W. Y.; Zheng, J. X.; Cheng, S. Z. D.; Li, C. Y.; Huang, P.; Zhu, L.; Xiong, H.; Ge, Q.; Guo, Y.; Quirk, R. P.; Lotz, B.; Deng, L.; Wu, C.; Thomas, E. L. Onset of Tethered Chain Overcrowding *Phys. Rev. Lett.* **2004**, *93*, 028301.
57. Sun, J.; Chen, X.; He, C.; Jing, X. Morphology and Structure of Single Crystals of Poly(ethylene glycol)–Poly(ε-caprolactone) Diblock Copolymers *Macromolecules* **2006**, *39*, 3717-3719.
58. Kundu, C.; Dasmahapatra, A. K. Effect of Block Asymmetry on the Crystallization of Double Crystalline Diblock Copolymers. *J. Chem. Phys.* **2014***, 141*, 044902.
59. Gan, Z.; Jiang, B.; Zhang, J. Poly(e-caprolactone)/Poly(ethylene oxide) Diblock Copolymer. II. Nonisothermal Crystallization and Melting Behavior *J. Appl. Polym. Sci.* **1997**, *63*, 1793-1804
60. Bogdanov, B.; Vidts, A.; Schacht, E.; Berghmans, H. Isothermal Crystallization of Poly(ε-caprolactone-ethylene glycol) Block Copolymers *Macromolecules* **1999**, *32*, 726-731
61. Piao, L.; Dai, Z.; Deng, M.; Chen, X.; Jing, X. Synthesis and Characterization of PCL/PEG/PCL Triblock Copolymers by Using Calcium Catalyst *Polymer* **2003**, *44*, 2025-2031
62. (a) Smallwood, I. *Handbook of Organic Solvent Properties*; Arnold: Great Britiain, 1996 (b) Wohlfarth, C. *Polymer Solutions*. Springer, New York, NY, 2010.
63. Mihailov, M.; Nedkov, E.; Goshev, I. Temperature Dependence of Morphology of Supermolecular Structures Growing in the Thin Layer Melt of Fractions of Poly(ethylene oxide). *J. Macromol. Sci. Phys. B* **1978**, *15*, 313-328
64. Van Horn, R.M.; Cheng, S.Z.D. Crystallization in polymer thin films: Morphology and growth. In *Polymer Thin Films*; Tsui, O.K.C. and Russell, T.P., Eds.; World Scientific: Rivers Edge, New Jersey, 2008.

SYNOPSIS TOC (Word Style “SN_Synopsis_TOC”). If you are submitting your paper to a journal that requires a synopsis graphic and/or synopsis paragraph, see the Instructions for Authors on the journal’s homepage for a description of what needs to be provided and for the size requirements of the artwork.

Authors are required to submit a graphic entry for the Table of Contents (TOC) that, in conjunction with the manuscript title, should give the reader a representative idea of one of the following: A key structure, reaction, equation, concept, or theorem, etc., that is discussed in the manuscript. Consult the journal’s Instructions for Authors for TOC graphic specifications.

